



Quantitative interpretation of potential field data in parts of Sakoli and Sausar fold belt in MP and Maharashtra, Central India

A. Kant^{1,2}, R. Kumar¹, U. Shankar², C.B. Tiwari³, S.R. Baswani⁴, R. Gorle⁵, A. Kumar⁶, S.K. Bharati³ and P.K. Jain⁶

¹Geological Survey of India, Central Region, Nagpur, India

²Department of Geophysics, BHU, Varanasi, India

³Geological Survey of India, Northern Region, Lucknow, India

⁴Geological Survey of India, SR, SU: AP, Hyderabad, India

⁵Geological Survey of India, M & CSD, Visakhapatnam, India

⁶Geological Survey of India, Western Region, Jaipur, India

abhayknt779@gmail.com

Available online at: www.isca.in

Received 22th March 2022, revised 2nd May 2023, accepted 26th June 2023

Abstract

The present study is intended for quantitative interpretation of gravity and magnetic data over Sausar and Sakoli belts in Madhya Pradesh and Maharashtra States, Central India. The gravity and magnetic data are used for the study were acquired under National Geophysical Mapping (NGPM) program of Geological Survey of India (GSI) covering an area of 6300 Km² during field season period 2012-14. The Sakoli and Sausar fold belts are the main structural domains in the area and well known for polyphase deformation activities. The metallic and non-metallic mineralization occurrences are also reported in these structural domains. The important feature, Central India Shear (CIS), demarcated as lineament F6-F6' is observed as steep gradient in Bouguer gravity anomaly map. Radially average power spectrum (RAPS) analysis of the gravity and magnetic data may be suggested average depth of basement around 4.5 Km and average depth of Sakoli and Sausar belts around 1.25 Km.

Keywords: Potential field, quantitative interpretation, Sakoli and Sausar fold belt, density and magnetic susceptibility.

Introduction

In exploration geophysics, gravity and magnetic methods, so-called potential field data, are often used. Interpretation is currently based on modeling and interpretation of collected data. The data are the values of the vertical component of gravity and total magnetic field. Measured data provide an excellent opportunity to more accurately map subsurface structures. Data is usually collected on the surface (ground) or on-board airplane (airborne). The potential field techniques are useful for mapping subsurface features such faults, fractures, shear zones, and altered zones that are important locations for the occurrence of mineral resources or the emplacement of an intrusive suite of rocks^{1,2}. The study area for the investigation is parts of Sakoli and Sausar belts in the Nagpur and Bhandara districts of Maharashtra and Balaghat district of Madhya Pradesh (Figure-1). The study area falls in Survey of India top sheet nos. 550/06, 07, 08, 10, 11, 12, 14, 15 & 16 at 1:50,000 scales, located between latitudes 21⁰⁰'00''N to 21⁰⁴'5'00''N and longitudes 79⁰'15'00''E and 80⁰'00'00''E.

Geology: The stratigraphy of litho-units ranges from age Archean to Paleoproterozoic to Neoproterozoic to Upper Cretaceous to Paleocene to Cenozoic. The study area is comprised by the oldest Tirodi Gneissic Complex/ Amgaon Gneissic Complex of Archean age, Sakoli and Sausar groups of

Paleoproterozoic age, Lameta Group of Upper Cretaceous age, Deccan Trap Supergroup of Upper Cretaceous to Paleocene age and Laterite of Cenozoic age (Figure-2 and 3).

Tirodi Gneissic Complex consists of two litho-units: amphibolite and gneiss which cover the major portion of the area. Tirodi Biotite Gneiss is a multi-component gneissic complex and it consists of a variety of gneisses like biotite-plagioclase gneiss, cordierite gneiss, tonalite gneiss etc. Tirodi Gneissic Complex forms the basement for the Sausar Group and patches of this are exposed in the form of inliers within the Sausar Group^{3,4}. The Amgaon Gneissic Complex is comprised of a wide range of litho units such as: quartzite, mica schist, kyanite-sillimanite-cordieriteschist, calc silicate, granulite, amphibolite, tonalite-trondhjemite granite/granodiorite, granite gneiss/migmatites, tourmalinite and vein quartz. The gneisses of Amgaon Gneissic Complex comprises of augen gneisses, streaky and banded gneisses. These gneisses are generally quartzo feldspathic in nature and may contain varying amounts of biotite, epidote, garnet, allanite, sphene, zircon and iron ores. Amgaon Gneissic Complex hosts and act as the basement for the Sakoli Group of rocks^{5,6}. Sausar Group is further divided into four formations in chronological order: Sitasongi, Lohangi, Mansar and Chorbaoli formations. Sitasongi Formation is characterized by arenaceous to argillaceous facies. It is comprised of quartzite and quartz-muscovite schist.

The quartzites and associated schists occur as linear bands⁷. Lohangi Formation is composed of calcareous meta-sediments viz. calc-gneiss, marble (dolomitic and calcitic). The Marble consists of calcite and dolomite as the main mineral with tremolite, epidote and serpentine as minor phase. The overlying Mansar Formation is represented by biotite schist, muscovite schist hosting stratiform Manganese (Mn) ore and Gondites with quartzite and thin dolomitic marble bands. Chorbaoli formation is characterized by quartzite and/or interbanded muscovite schist/quartzite garnetiferous quartz mica schist meta-arkose with local development of magnetite and/or garnet⁸.

The Sakoli Group is intruded by quartz vein/silicified zone, granite/pegmatite and vein quartz of Palaeoproterozoic Age. Sakoli Group represents the litho units of Gaikhuri, Dhabetekri and Bhiwapur formations. Gaikhuri Formation is comprised of conglomerate, gritty quartzite with minor pelites and Banded

Iron Formation (BIF). Dhabetekri Formation is mainly composed of meta-basalt with subordinate meta-pelites, chertbands and meta-ultramafic rocks. Bhiwapur Formation is characterized by interbands of metamorphosed acid volcanics/tuffs of rhyolite to rhyodacite composition, minor psammites, exhalative sediments, coticule, tourmalinite, meta-rhyolite and tuff. The sediments of Lameta Group are non-fossiliferous. The limestone of Lameta Group in the area shows sub-horizontal disposition^{5,9-11}. The Deccan Trap Super group is represented by basaltic flows of Amarkantak and Satpura groups. The flow types vary from 'pahoehoe' to 'aa' and there is also a transition from pahoehoe to 'aa' flow. All the flows are fine grained, compact and sparsely porphyritic. Amarkantak Group consists of 'aa' type single basaltic flow in the area. Laterite occurs as isolated capping on the Deccan Trap lava flows especially on the upper most part of Amarkantak Group⁵.

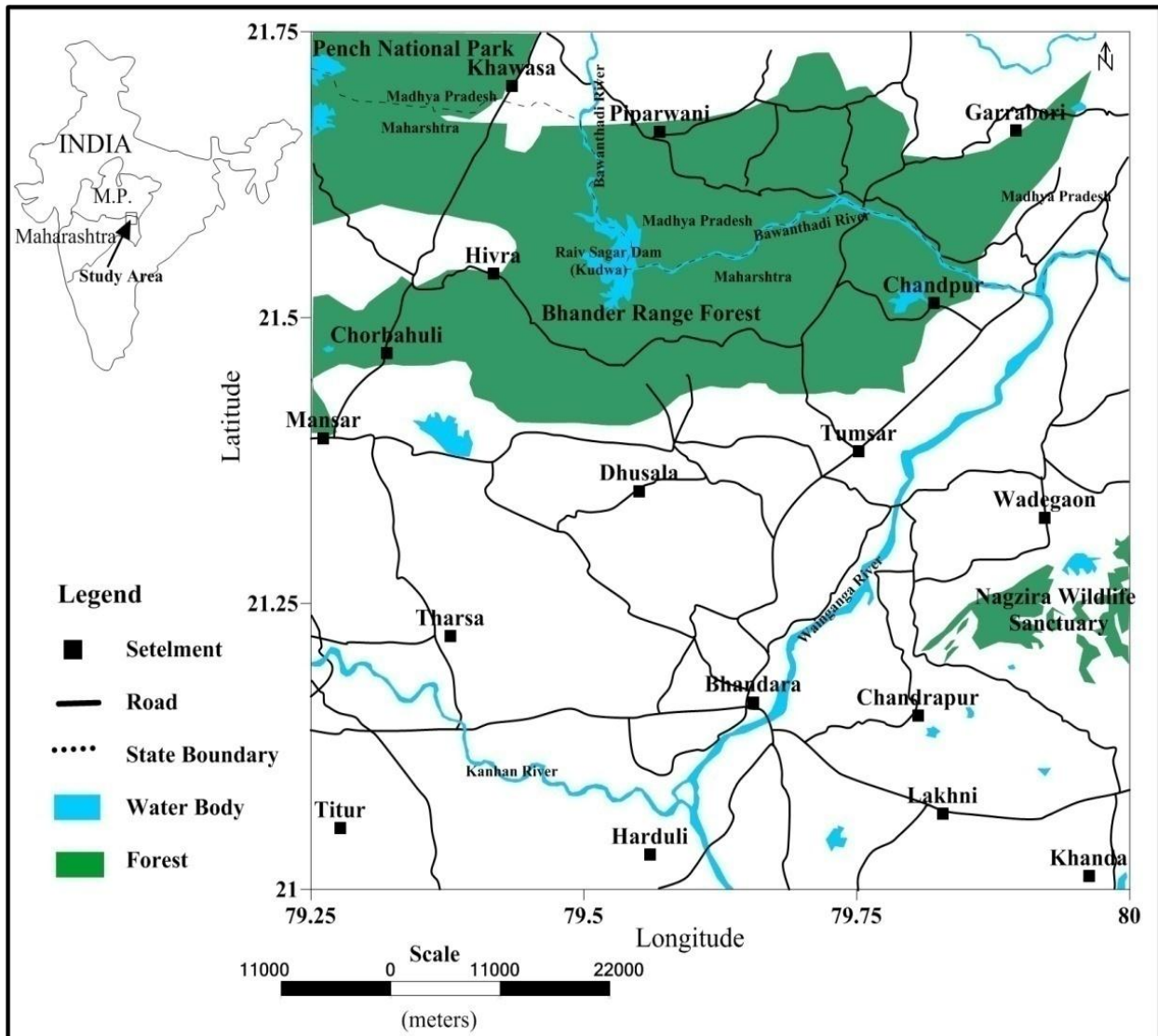


Figure-1: Location map of the study area.

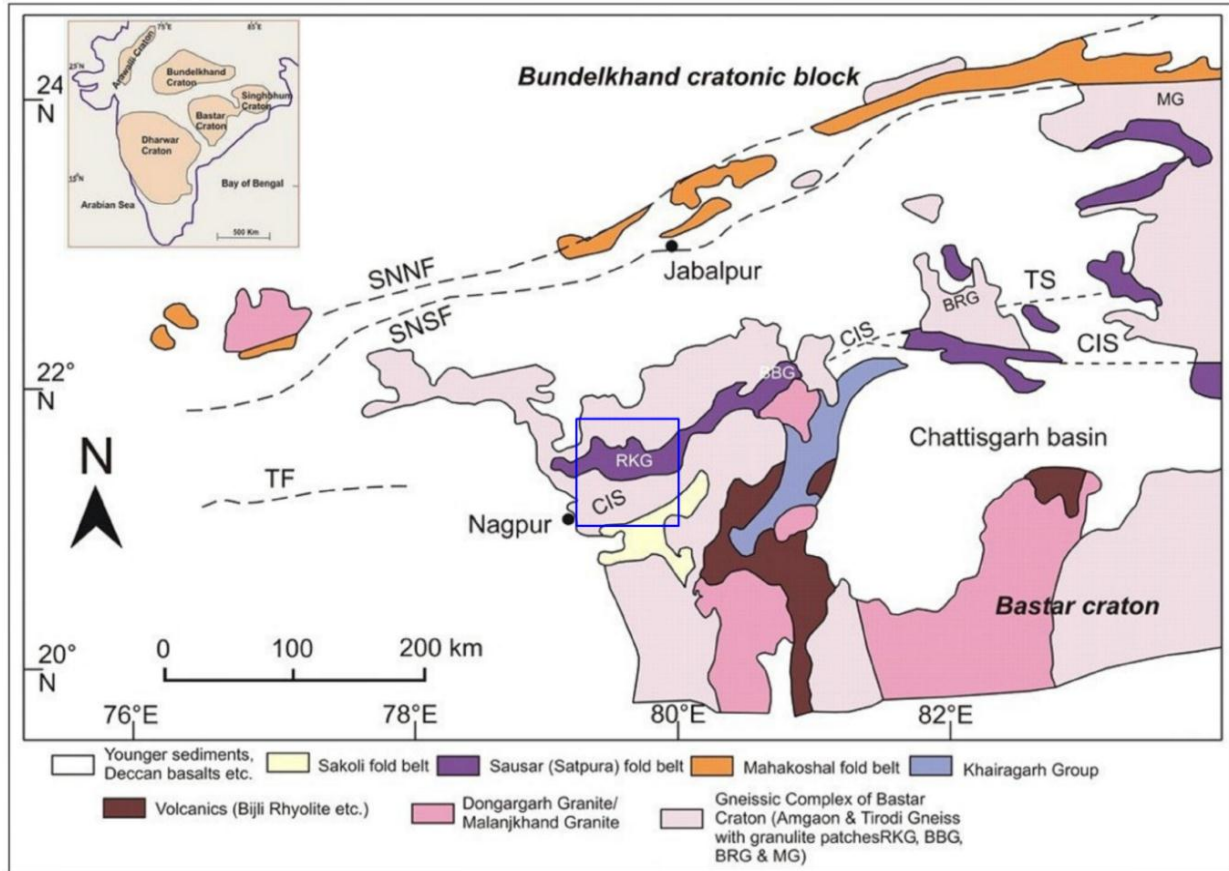


Figure-2: Regional geological map of Sakoli and Sausar Belt of study area¹²⁻¹⁹.

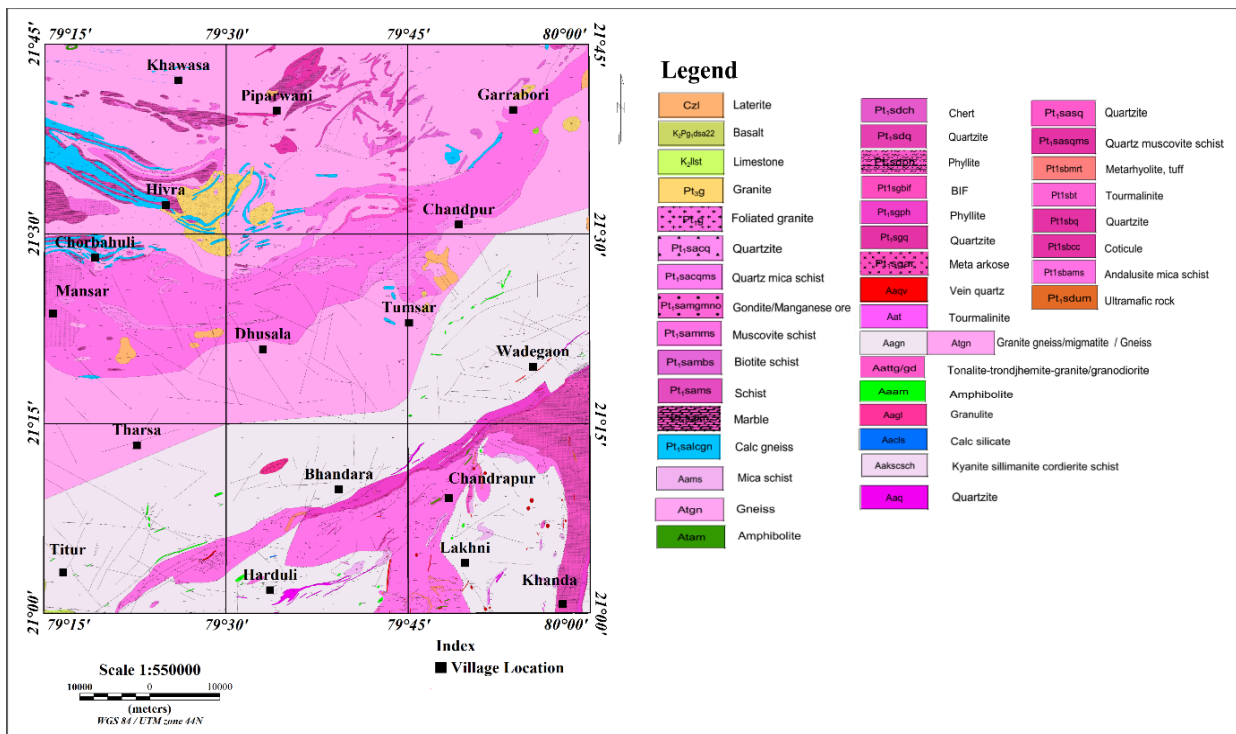


Figure-3: Local geology map of Study area²⁰.

Methodology

Gravity, Magnetic and Differential Global Positioning System (DGPS) data were acquired by deploying Scintrex CG-5 Autograv gravimeter (resolution 0.001 mGal), GSM-19T Magnetometer (resolution 0.01nT) and Leica Geosystem DGPS 1200 (resolution 5-10 mm) respectively. A total of 2520GM (Gravity and magnetic) points were observed with a station density of 1 GM station per 2.5 sq. km across the entire study area of 6300 sq. km (Figure-4). GM observation points along with DGPS were observed along the available roads, forest tracks, cart tracks and foot tracks with a station spacing varying between 1.25 and 1.50Km and away from the high-rise buildings, electric lines, bridges, power line and electricity pole etc. The 1980 Geodetic Reference System (GRS80) is used to calculate the theoretical gravity at each observation points. To get the Bouguer anomaly values at each location, the raw gravity data were subjected to instrument drift (based on repeated observations), Free-air, and Bouguer adjustment. To obtain total field magnetic anomaly values, the International Geomagnetic Reference Field (IGRF) correction was subjected to diurnally adjusted magnetic data using IGRF coefficients for the 2015 epoch²¹⁻²³.

Results and Discussion

Bouguer Gravity Anomaly Contours with Density of Rocks Samples overlaid on Geological Map: Bouguer gravity anomaly values are gridded and contoured by using minimum curvature module of Oasis Montaj Geosoft programs, to produce the Bouguer gravity anomaly map, which is indicated various anomalous zones. The Bouguer gravity anomaly contour (Figure-5) along with density value of rock samples are overlaid on geological map of study area (Figure-6) for better understanding of geophysical responses with the geological

features / litho contacts / lineaments. Bouguer gravity anomaly contour map is implied broad gravity variations such as gravity 'high' in northern and southern portion whereas 'low' is recorded in central part of study area. Surface exposure of high density rock over gravity high "H1" is not much visible except few high density samples of and Phyllites (Density~3.1 gm/cc) of Sakoli Group of rocks within the Tourmalinites, Amphibolites, high-grade mica schist and Granite gneiss/migmatites of Amgaon Gneissic Complex. Gravity high "H2" is recorded over andalusite mica schist, coticule (quartz-spessartine garnet rock) of Sakoli Group. In the report GSI 2017, the Amgaon Gneissic Complex and Sakoli contained by Granite, pegmatite and quartz veins. The epigenetic tungsten mineralization i.e. scheelite and wolframite is associated with granitoid/ pegmatite greisen zones. Gravity high "H3" is recorded near Khawasa, Piparwani and Hivra villages in northern portion of the area and implies high density rocks (density~2.85 gm/cc) e.g. marble, gneisses, schist and quartz muscovite schist of Sausar Group underlying in the gneisses of Archean Tirodi Gneissic Complex. The metamorphic mineral assemblages of calc-silicate and meta-pelites of Sausar Group indicating amphibolite facies of metamorphism contributing to the higher density. High density Manganese ore deposits hosted by meta-sediments of Mansar Formation of the Sausar Group is also lying in the surroundings of the gravity high "H3". The gravity 'high' (H4) is observed around Garrabori villages in northeastern portion area which is due the cumulative effect of magnetite-quartzite, calc-granulites, muscovite-biotite schist, quartz-muscovite schist and quartz-biotite schist of Lohangi and Mansar formations of Sausar Group. Gravity low "L1" is recorded over comparatively low density (~2.63gm/cc) rock of Tirodi Gneissic Complex. Tirodi Gneissic Complex comprises a variety of gneissic rocks viz., biotite-plagioclase gneiss, felsic-migmatitic gneiss, tonalitic gneiss, cordierite gneiss.

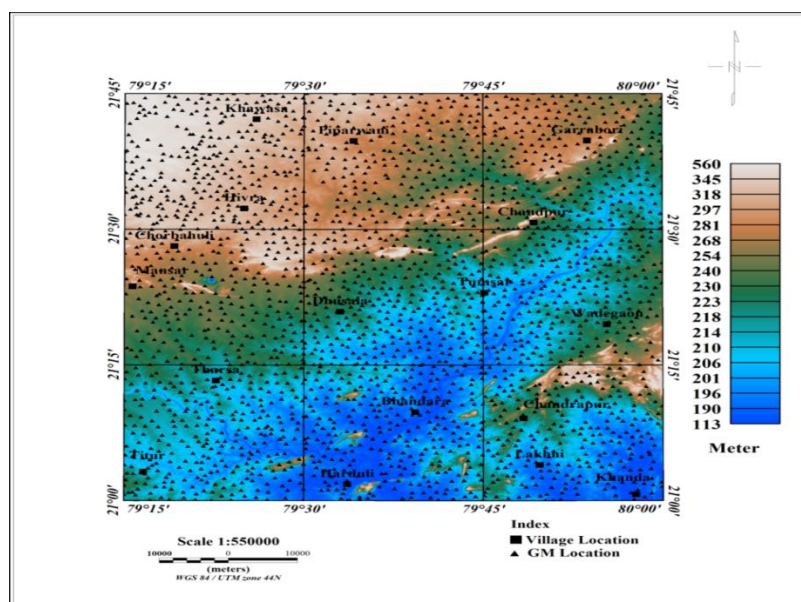


Figure-4: GM points overlaid on Digital elevation model (DEM)²⁴.

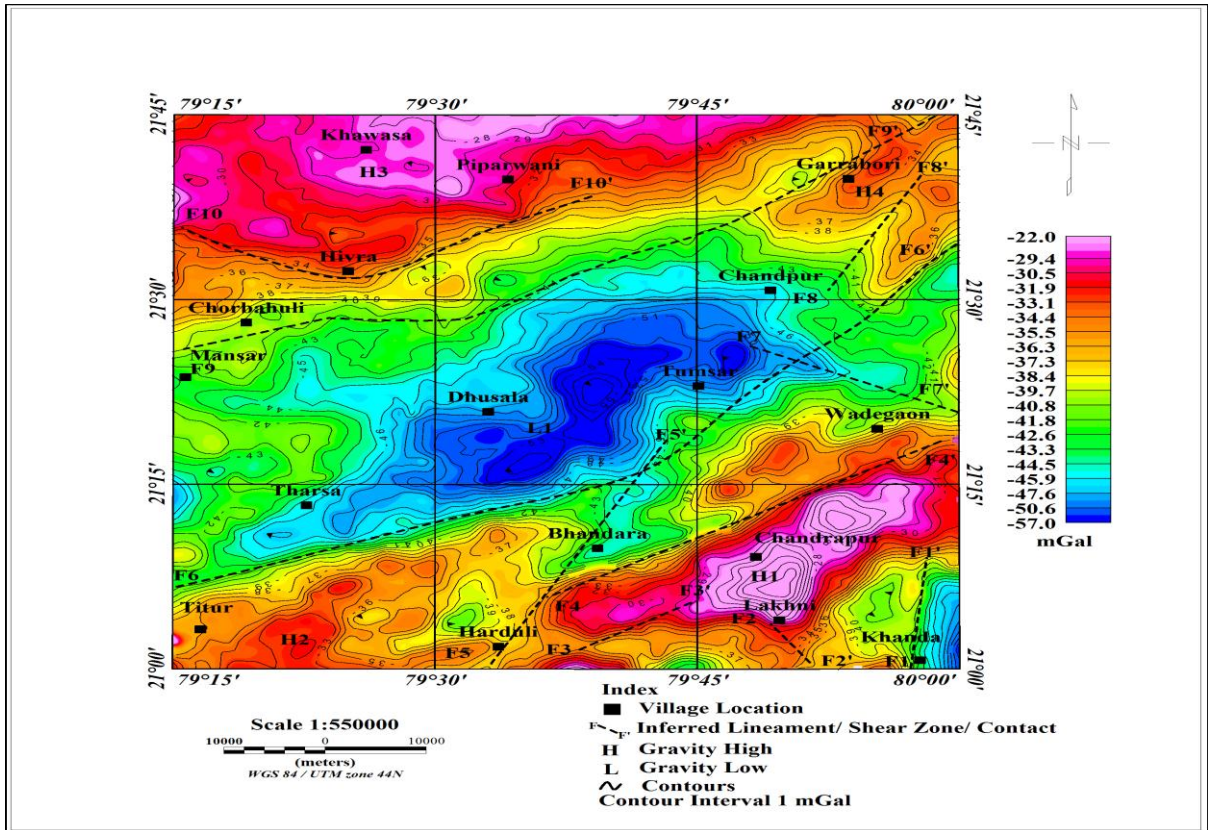


Figure-5: Bouguer gravity anomaly contour map.

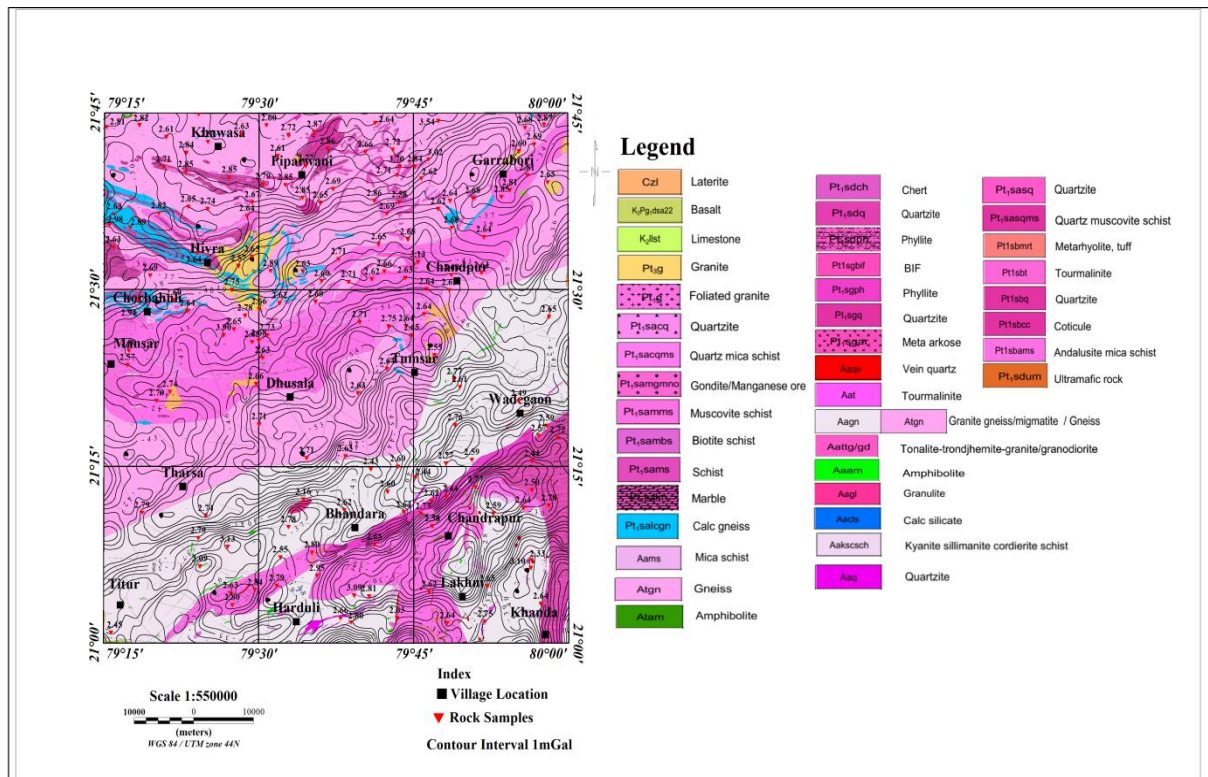


Figure-6: Bouguer gravity anomaly contour with density of rocks samples overlaid on geological map.

Magnetic (T.F.) Anomaly Contours with Magnetic Susceptibility of Rocks Samples overlaid on Geological Map:

The contours of magnetic anomaly (Figure-7) along with magnetic susceptibility values of rock samples are overlaid on geological map shown in Figure-8 for better understanding of magnetic response of the geological features/ litho contacts/ lineaments. The high intensity magnetic anomalies around Titur, Harduli and Chandrapur are observed over comparatively higher magnetic susceptibility rocks Andalusite mica schist and Phyllite of Sakoli Group. The high intensity magnetic anomalies around Khawasa and Hivra are recorded over magnetite-quartzite, manganese-rich biotite, muscovite-biotite schist, quartz-muscovite schist, quartz-biotite schist of Sausar Group and gneisses & amphibolites of Tirodi Gneissic Complex. Moderate intensity magnetic anomalies in the south of Piparwani and north of Tharsa are recorded over Cenozoic Laterite, Neoproterozoic granite, Calcareous gneiss of Sausar Group and basement gneisses of Tirodi Gneissic Complex. The Low intensity magnetic anomalies near Dhusala are characterizing the less magnetic susceptible gneisses of Tirodi Gneissic Complex and Muscovite schist of Sausar Group.

Radially Average Power Spectrum (RAPS): RAPS of gravity data is presented in Figure-9. The power spectrum implies three linear slope segments and estimates the density interfaces at depths viz., 0.57Km (shallow), 1.34Km (intermediate) and 4.48 Km (deeper). The deeper subsurface density interface at a depth of 4.48Km may be indicating the average depth of basement rocks, whereas the density interface at 1.34Km may be

indicating mean average depth of Sausar and Sakoli meta-sediment. The shallow density interface at a depth of 0.57Km may be due to the amphibolites and meta-basalt. The RAPS plot of magnetic data (Figure-10) is also interpreted as three linear slope segments. The magnetic interfaces at depths, viz. 0.4Km (shallow), 1.15Km (intermediate) and 4.56Km (deeper). The magnetic interface at a depth of 4.56Km may imply the average depth of basement, whereas the interface at a depth of 1.15Km may be indicating the depth of Sausar and Sakoli meta-sediment. Shallow magnetic interface at a depth of 0.4 Km may be due to the amphibolites and meta-basalt.

Euler 3D Depth Solutions: The Euler 3D deconvolution technique is based on Euler's homogeneity equation, which is related to estimate the depth of causative sources from potential field data and its first order gradient components in three directions to the location of the data sources and gridded data with the degree of homogeneity, which may be interpreted as a structural index (SI). The SI is a measurement of the rate at which the anomaly changes with distance from the source and is based on the geometry of the potential field data²⁵. Euler solutions of gravity data are calculated with window size = 15 Km, depth tolerance = 15, and SI = 0 values to highlight the contacts and faults illustrated in Figure-11. The inferred fault, boundary, tectonic contact, and contact between two litho-units, which vary in depth from 1.0 to 2.0km, are where the Euler 3D solution of gravity data is falling.

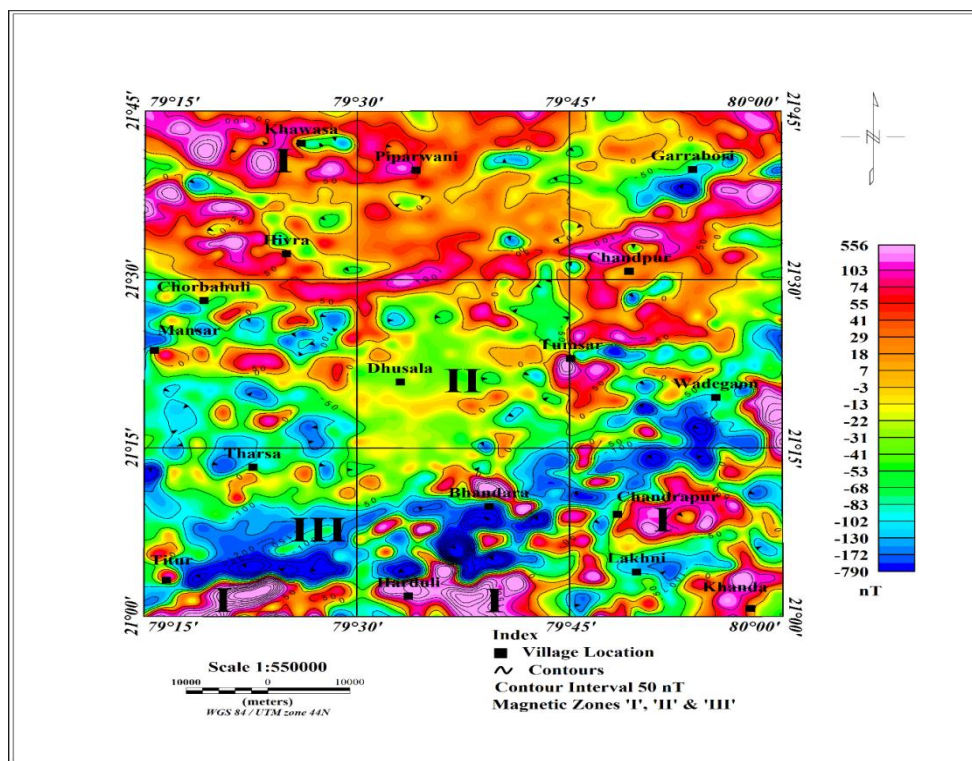


Figure-7: Magnetic anomaly contour map.

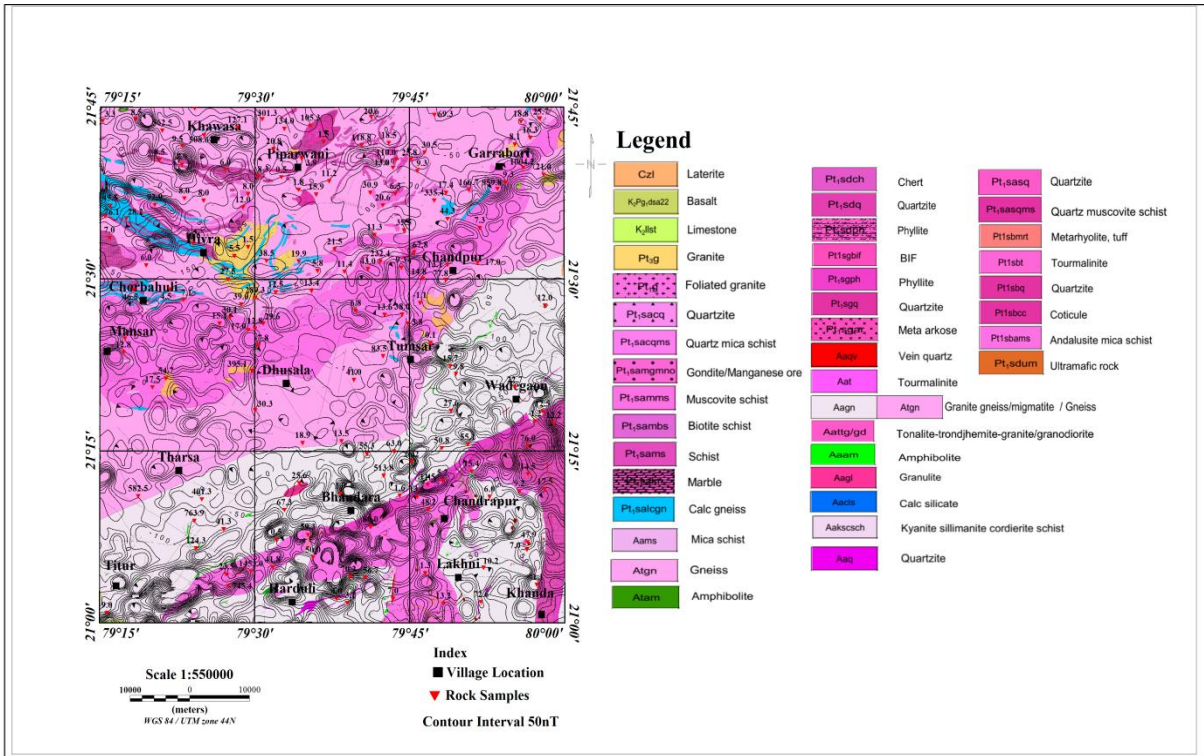


Figure-8: Magnetic anomaly contour with magnetic susceptibility of rocks samples overlaid on geological map.

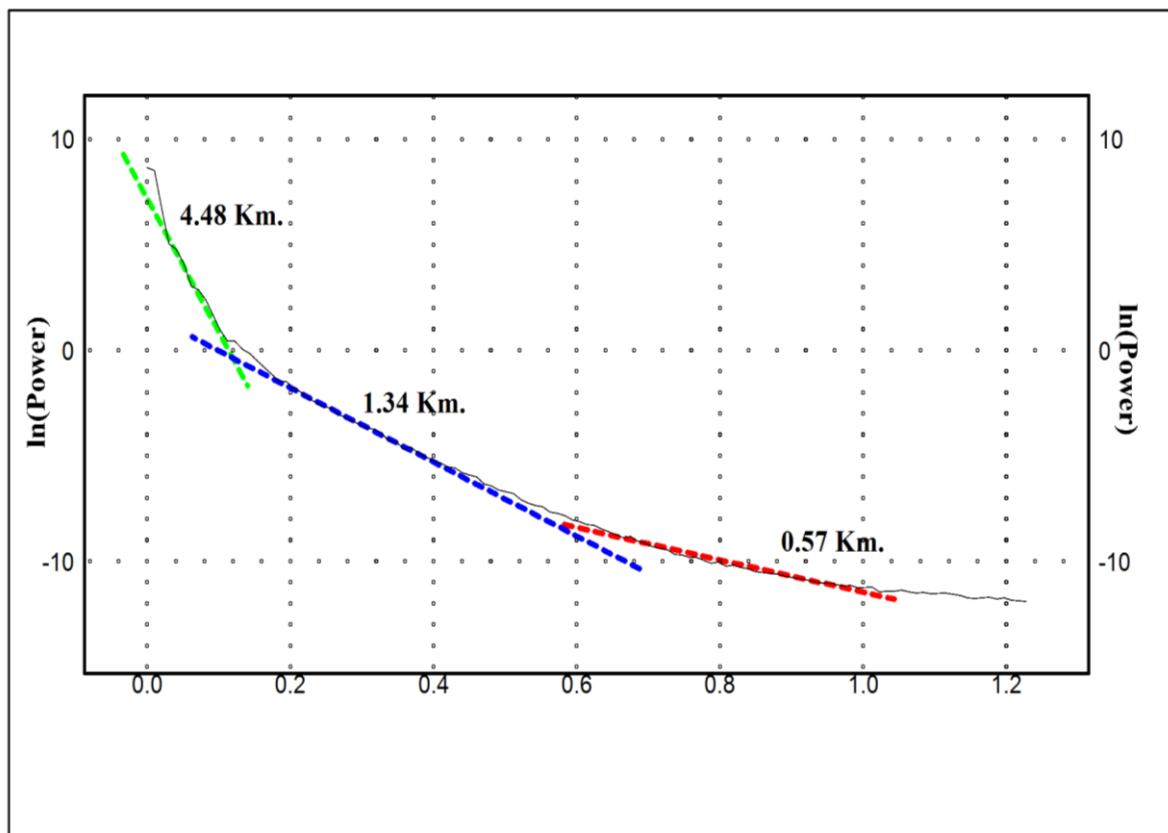


Figure-9: RAPS of Bouguer gravity anomaly.

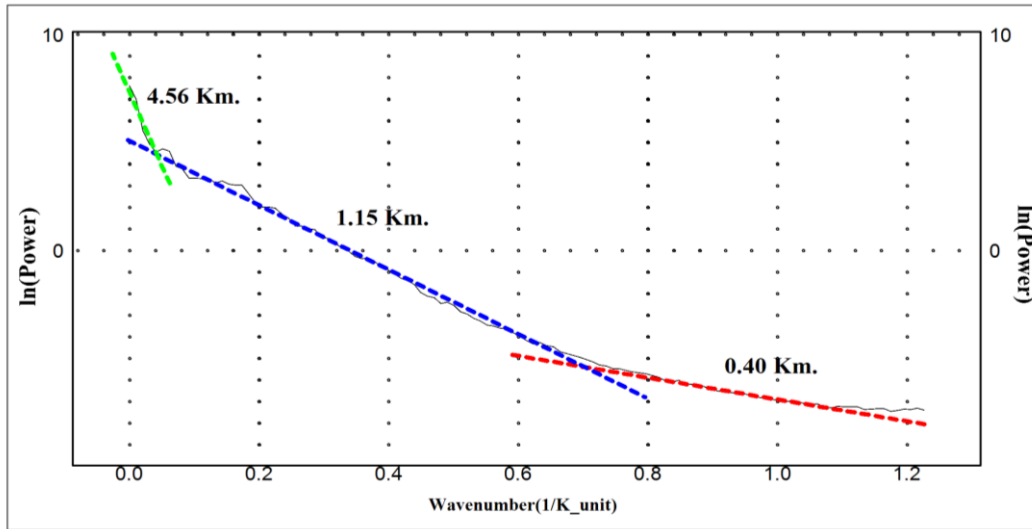


Figure-10: RAPS of magnetic anomaly.

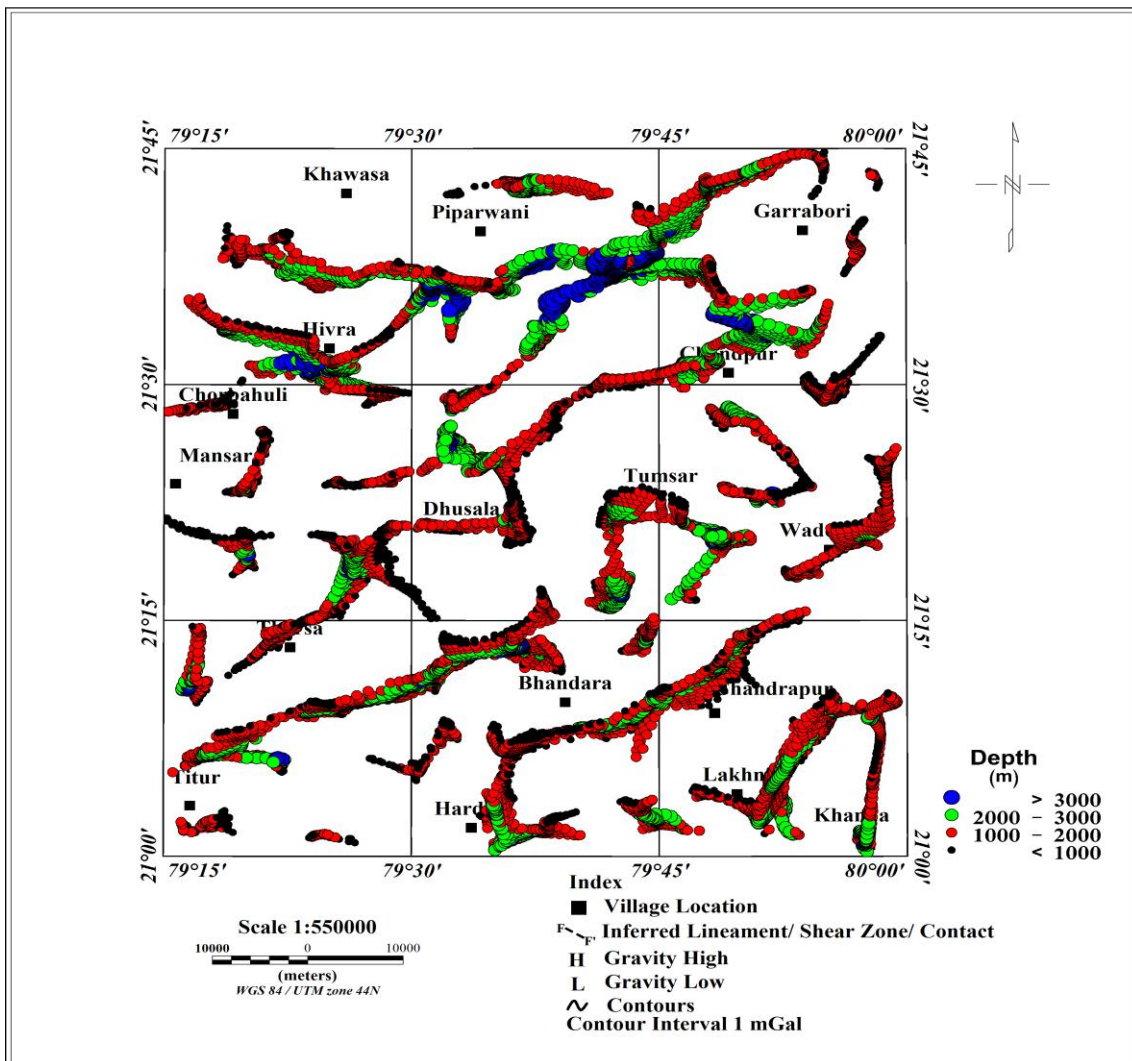


Figure-11: Euler 3D depth solutions gravity data.

Density and Magnetic Susceptibility Measurements of Rock Samples: A total of 159 rock samples are taken during fieldwork from various litho-units. A density metre made by Mettler Toledo (ME 403) was used to gauge the density of rock samples. Rock samples' magnetic susceptibilities were assessed using a Bartington Instruments Limited, UK-made MS-2 (Dual Frequency) Magnetic Susceptibility metre (MS 2B). Table-1 lists the measured densities and magnetic susceptibilities of rock samples. It is observed that quartzite, quartz mica schist, pegmatite and foliated granite are having low density and low to

moderate magnetic susceptibility order. Whereas, amphibolite, Mn ore, iron ore and garnet pyrope are characterized by high density and moderately high magnetic susceptibility. Phyllite and basic rocks can be characterized by moderately high density and very high magnetic susceptibility. Gneiss, marble and granite are showing moderate density and moderate susceptibility. The physical processes viz. alteration/ weathering can change the physical properties of the rocks as in the case of magnetic susceptibility of quartzite and foliated quartzite.

Table-1: Physical properties of rock samples.

Rock Type	No. of Samples	Density gm/cc		Susceptibility X10 ⁻⁶ CGS Units	
		Range	Average	Range	Average
Amphibolite	2	2.808 - 3.128	2.968	9.25 - 41.3	25.3
Basic Rock	1	2.949	2.949	421.3	421.3
Biotite schist	1	2.804	2.804	17.4	17.4
Calc Gneiss	2	2.717 - 2.894	2.806	6.5 - 38.5	22.5
Calc Silicate	9	2.625 - 3.112	2.843	0.5 - 154.3	45.3
Dyke	1	3.128	3.128	44.5	44.5
Foliated Granite	5	2.575 - 2.859	2.665	6.3 - 55	24.2
Foliated Quartzite	1	2.646	2.646	7.6	7.6
Garnet Pyrope	1	3.701	3.701	110	110
Gneiss	48	2.525 - 3.085	2.714	2.2 - 232.5	34.5
Granitic Gneisses	2	2.6 - 2.891	2.745	13.55 - 28.2	20.775
Granite	5	2.601 - 2.664	2.83	1.5 - 301.25	73.36
Iron ore	1	3.064	3.064	59	59
Laterite (iron rich)	1	3.102	3.102	49.1	49.1
Manganese	1	3.539	3.539	69.25	69.25
Manganiferous Qtz Mica Schist	1	2.63	2.63	7.8	7.8
Marble	9	2.627 - 2.869	2.789	2.7 - 253	38.5
Mn bearing Quartzite	2	3.015 - 3.134	3.075	30.5 - 67.75	49.1
Mn ore	1	3.903	3.903	15.1	15.1
Muscovite Schist	6	2.623 - 2.848	2.718	6 - 1004.2	339.5
Pegmatite	11	2.567 - 2.752	2.635	8 - 508.6	97.5
Phyllite	8	2.737 - 2.836	2.799	45 - 1453	679.2
Qtz Mica Schist	3	2.619 - 2.754	2.698	8.4 - 18.5	13.5
Quartz	7	2.625 - 2.85	2.667	7.9 - 63.2	25.5
Quartz Vein	7	2.632 - 2.683	2.653	9.25 - 289.3	102.5
Quartzite	20	2.45 - 2.848	2.653	0.75 - 562.5	58.3
Schist	2	2.664 - 2.737	2.701	54.7 - 395.1	224.9
Tourmaline	1	2.836	2.836	25.75	25.75

Conclusion

The analysis of power spectrum of gravity and magnetic data provides approximately same depth interfaces. The deeper subsurface interface at a depth of 4.48Km may be indicating the average depth of basement rocks, whereas the intermediate interface at 1.34Km may be indicating mean average depth of Sausar and Sakoli meta-sediment. The shallow density interface at a depth of 0.57Km may be due to the amphibolites and metabasalt. The Euler depth solutions generated from gravity data suggest the source depth of most of the lineaments varying the depth from 1.0 to 2.0Km.

Acknowledgement

We would like to thank to Dr. J. Rajeshwar, ADG & HoD, GSI, CR, Nagpur for providing the Infrastructure to complete this work. We are thankful to the reviewers and editor of the journal who have given critical and

References

1. Dahanayake, K., & Subasinghe, S. M. N. D. (1988). Development of recent stromatolitic structures and phosphatic enrichment in Precambrian marble of Sri Lanka. *Economic Geology*, 83(7), 1468-1474.
2. Subasinghe, N. D. (1998). Formation of a phosphate deposit through weathering and diagenesis—an example from Sri Lanka. (Doctoral dissertation, PhD Thesis (Unpubl.) University of Reading).
3. Basu, N.K. (1958). On the stratigraphy and structure of the Sausar Series of Mahuli-Ramtek area, Nagpur district, Bombay. *Quarterly journal of the Geological, Mining, and Metallurgical Society of India*, 5(30), 39-41.
4. Mohanty, S.P. (1993). Stratigraphic position of the Tirodi gneiss in the Precambrian terrane of central India: evidence from the Mansar area, Nagpur district, Maharashtra. *Journal of Geological Society of India*, 41(40), 55-60.
5. Yedekar, D.B., Karmalkar, N., Pawar, N.J. and Jain, S.C. (2003). Tectonomagmatic evolution of Central Indian terrain. *Gondwana Geological Magazine*, 7, 67-88.
6. Wanjari N. and Ahmad T. (2007). Geochemistry of Granitoids and Associated Mafic Enclaves in Kalpathri Area of Amgaon Gneissic Complex, Central India. *Gondwana Geological Magazine*, 10, 55-64.
7. Basu N.K. and Sarkar S.N. (1966). Stratigraphy and structure of the Sausar Series in the Mahuli-Ramtek-Junawani area, Nagpur district, Maharashtra. *Quarterly journal of the Geological, Mining, and Metallurgical Society of India*, 5(38), 77-105.
8. Mohanty S. (1988). Structural evolution of the southern part of the Sausar belt near Ramtek, Nagpur district, Maharashtra. *Indian Journal of Geology*, 3(60), 200-210.
9. Rao G.V. (1970). The geology and manganese-ore deposits of the manganese belt in Madhya Pradesh and adjoining parts of Maharashtra. Part II - The geology and manganeseore deposits of Kanhan-Pench valley area, Nagpur district, Maharashtra and Chhindwara district, Madhya Pradesh. *Bulletin of Geological Survey of India*, 5(A-22, II), 1-100.
10. Straczek, J. A. (1956). Manganese ore deposits of Madhya Pradesh, India, Symposium Sobre Yacimientos De Manganeso. In Toma IV. Asia Oceania. XX Congreso Geologico Internacional Mexico (pp. 63-96).
11. Subramanyam M.R. (1972). The geology and manganese ore deposits of the manganese belt in Madhya Pradesh and adjoining parts of Maharashtra. Part VI - The geology and manganese deposits of Ramrama-Sonawani area, Waraseoni Tahsil, Balaghat district and parts of Seoni Tahsil, Chhindwara district, Madhya Pradesh. *Bulletin of Geological Survey of India*, 5(A-22,VI), 1-53.
12. Mohanty N., Singh S.P., Satyanarayanan M., Jayananda M., Korakoppa M.M. and Hiloidari S. (2018). Chromian spinel compositions from Madawara ultramaBcs, Bundelkhand Craton: Implications on petrogenesis and tectonic evolution of the southern part of Bundelkhand Craton, central India. *Geological Journal*, 54, 2099-2123.
13. Saha D. and Mazumder R. (2012). An overview of the Palaeoproterozoic Geology of Peninsular India, and key Stratigraphic and Tectonic Issues. *Geological Society of London*, 365, 5-29, <https://doi.org/10.1144/sp365.2>.
14. Stein H., Hannah J., Zimmerman A. and Markey R. (2006). Mineralization and deformation of the Malanjkhland terrane (2,490–2,440 Ma) along the southern margin of the Central Indian Tectonic Zone. *Mineralium Deposita*, 40, 755-765.
15. Sarkar S.N., Trivedi J.R. and Gopalan K. (1986). Rb–Sr whole rock and mineral isochron age of the Tirodi gneiss, Sausar Group, Bhandara district, Maharashtra. *Geological Society of India*, 27, 30-37.
16. Bhowmik S.K., Wilde S.A. and Bhandari A. (2011). Zircon U–Pb/Lu–Hf and monazite chemical dating of the tirodi biotite gneiss: implication for Latest Paleoproterozoic to Early Mesoproterozoic Orogenesis in the Central Indian Tectonic Zone. *Geological Journal*, DOI:10.1002/gj.1299.
17. Pandey B.K., Krishna V. and Chabria T. (1998). An overview of Chhota nagpur gneissgranulite complex and adjoining sedimentary sequences, Eastern and Central India, International seminar on Precambrian crust in eastern and central India: *UNESCO-International Union of Geological Sciences. International Geoscience Programme-368*, 131-135.
18. Roy A., Kagami H., Yoshida M., Roy A., Bandyopadhyay B.K., Chattopadhyay A., Khan A.S., Huin A.K. and Pal, T. (2006). Rb–Sr and Sm–Nd dating of different metamorphic events from the Sausar Mobile Belt, central India:

- Implications for Proterozoic crustal evolution. *Journal of Asian Earth Sciences*, 26, 61-76.
19. Lippolt H.J. and Hautmann S. (1995). $^{40}\text{Ar}/^{39}\text{Ar}$ ages of Precambrian manganese ore minerals from Sweden, India and Morocco. *Mineralium Deposita*, 30, 246–256.
 20. GSI (2017). Geological survey of India. <https://bhukosh.gsi.gov.in/Bhukosh/Public>.
 21. Baranov V. (1957a). A new method for interpretation of aeromagnetic maps: Pseudogravimetric anomalies. *Geophysics*, 22, 359-383.
 22. Roest, Walter R. and Pilkington, Mark (1993). Identifying remanent magnetization effects in magnetic data. *Geophysics*, 58 (5). 653-659.
 23. Mandal A., Chandroth A., Basantaray A.K. and Mishra U. (2020). Delineation of shallow structures in Madawara igneous complex, Bundelkhand Craton, India using gravitymagnetic data: Implication to tectonic evolution and mineralization. *Journal of Earth System Science*, 129(90), 1-17.
 24. Bhuvan (2021). Indian Geo-Platform of ISRO. <https://bhuvan-app3.nrsc.gov.in/data/download/index.php>, *SRTM data*, July 15, 2021.
 25. Thompson, D.T. (1982). EUIDPH: A New Technique for Making Computer-Assisted Depth Estimates from Magnetic Data. *Geophysics*, 47, 31-37.